II

Publication II

K. Mansikkamäki, U. Haapanen, C. Johans, K. Kontturi, M. Valden, Adsorption of Benzotriazole on the Surface of Copper Alloys Studied by SECM and XPS, *J. Electrochem. Soc.* **153** (2006) B311-B318.

Journal of The Electrochemical Society, **153** (8) B311-B318 (2006)
0013-4651/2006/153(8)/B311/8/$20.00 © The Electrochemical Society

Adsorption of Benzotriazole on the Surface of Copper Alloys Studied by SECM and XPS

K. Mansikkamäki,[a] U. Haapanen,[b] C. Johans,[a] K. Kontturi,[a,z] and M. Valden[b]

[a]*Laboratory of Physical Chemistry and Electrochemistry, Helsinki University of Technology, FI-02015 TKK, Finland*
[b]*Surface Science Laboratory, Tampere University of Technology, FI-33101 Tampere, Finland*

The formation of inhibitive benzotriazole films on copper and copper alloyed with silver has been studied with scanning electrochemical microscopy (SECM) and X-ray photoelectron spectroscopy (XPS). The SECM measurements showed that the film grows rapidly on oxygen-free dehydrated copper (OF-HC) and that the rate depends on the substrate potential. The benzotriazole films were also observed on silver alloyed copper; however, electropolishing prevents film growth by enriching the surface with silver. XPS results show that the film consisted of [Cu(I)–BTA] on both materials. No evidence of [Ag(I)–BTA] was found.
 [DOI: 10.1149/1.2208912]

Manuscript submitted February 21, 2006; revised manuscript received April 4, 2006. Available electronically June 13, 2006.

Copper is a widely used material in industry, mainly due to its good electrical and thermal properties as well as corrosion resilience. Several copper alloys have been developed for different applications. Oxygen-free dehydrated copper (OF-HC, < 10 ppm oxygen) is used in microelectronics, and CuAg (0.25% Ag) has been developed for electrical applications that require high strength at elevated operation temperatures.[1] Alloying elements generally decrease the electrical conductivity of copper, e.g., phosphorus has a significant influence even in the parts per million range;[2] however, copper alloyed with silver (CuAg) has only a minor effect on conductivity, even in high concentrations. Because OF-HC is mainly used in applications with high demands on electric and thermal conductivity, the amount of impurities and additives must be low.

Despite the good corrosion resistance of copper, oxidation may take place in some media, and inhibitors are needed.[2,3] Benzotriazole (BTAH) has been used as a corrosion inhibitor for over 50 years and its role is overwhelming.[3] BTAH is an anodic-type inhibitor,[4] even though it has been found to inhibit cathodic oxygen reduction.[5] The mechanism by which BTAH protects copper surfaces is still not known in detail. It is generally accepted that a [Cu(I)–BTA] complex is formed at the copper surface, which inhibits further oxidation. It has been shown that [Cu(I)–BTA] forms multilayers using Cu–N bonds[3,6,7] at open-circuit potential. However, the role of oxygen in the formation of the [Cu(I)–BTA] film[4-6,8-10] as well as the orientation and binding of BTAH molecules on the copper surface[5,11-13] have caused a lot of debate.

Both pH and potential affect [Cu(I)–BTA] film formation.[14-21] According to Youda et al.,[14] negative potentials are required for adsorption and film formation of BTAH in acidic solutions; however, in neutral solutions film formation occurs in the whole potential range. Yao et al.[15] studied adsorption of BTAH in acetonitrile solution with surface-enhanced Raman spectroscopy (SERS) and observed that BTAH adsorbed at negative potentials (−0.3–0 V vs Ag/AgCl) and that a polymeric [Cu(I)–BTA] complex film was formed at more positive potentials (0 − 0.2 V vs Ag/AgCl). Gao et al..[16] proposed that the composition of the [Cu(I)–BTA] film changes with potential. The polymeric complex film, $[Cu(I)–BTA]_n$, is converted to a $[Cu(I)–BTA]_4$ film at negative potentials [−0.5 to −1.1 V vs SCE] in neutral chloride solutions, because the lower potential results in lower pH at the electrode surface, which, on the other hand, results in decomposition of the $[Cu(I)–BTA]_n$ to $[Cu\ BTA]_4$. According to Chan and Weaver,[17] adsorbed BTAH molecules deprotonate on the copper surface when the potential is more positive than −0.3 to −0.2 V vs SCE and the pH greater than 2 in a solution of Na_2SO_4 and H_2SO_4. However, according to Schultz et al.,[18] BTAH adsorbs in a well-ordered manner in its deprotonated form, BTA^-, on Cu(100) in the whole potential region (−0.65 to 0.20 V vs Ag/AgCl), while on Cu(111) the layer is disordered at negative potentials.

Relatively few studies considering BTAH on silver surfaces have been published. Kapoor[22] has stabilized Ag nanoparticles using BTAH. He concluded that BTAH facilitates oxidation of the nanoparticles through a preoxidation mechanism induced by the nucleophilic character of BTAH. Thomas et al.[23] studied silver nanoparticle sols with SERS and found that a [Ag(I)–BTA] film was formed, where BTA is in an upright orientation. Additionally, theoretical calculations of Naumov et al.[24] indicate that a polymeric [Ag(I)–BTA] complex is energetically favorable on Ag nanoparticles. Ahn and Kim[25] have studied the effect of BTAH in superconformal electroplating of silver. They recorded that BTAH acts as an inhibitor on copper seed layers, as expected, but quite surprisingly, it acts as an accelerator on silver seed layers. This was explained in terms of the weak adsorption of BTAH on silver in comparison to copper.

Scanning electrochemical microscopy (SECM) provides an excellent tool for in situ study of film growth on various materials, while simultaneously controlling the potential of the substrate. SECM has, for example, been used to study defects in aluminum oxide,[26,27] redox-active sites on titanium,[28] and iodide oxidation at Ta/Ta_2O_5 electrodes.[29] We have previously used SECM to study the effect of BTAH on phosphorus-deoxidized (DHP) copper[21] and the influence of oxygen on the formation of the [Cu(I)–BTA] film.[30] Several X-ray photoelectron spectroscopy (XPS) studies of BTAH and copper have been conducted,[3,11,31-33] but studies of BTAH on silver surfaces using XPS have not been reported.

In this study we examine adsorption of BTAH on oxygen-free copper (OF-HC) and copper alloyed with silver (CuAg). The purpose was to study how the alloyed elements affect the formation of the inhibiting [Cu(I)–BTA] adlayer. SECM was used to follow the transition of the copper surface from conducting to insulating as film growth proceeds. The resulting approach curves are analyzed as reported earlier.[21] XPS was used to obtain information on the chemical state of the substrate surface, the inhibitive film, and the bonds formed in the adsorption process.

Experimental

SECM measurements.— The measurements were done in a three-electrode cell with a saturated calomel reference electrode (SCE) and a Pt counter electrode. All potentials reported in this work are referred to the SCE. The reference electrode was connected to the cell using a salt bridge to avoid chloride ion contamination. The SECM tip (working electrode) was prepared in-house and consisted of a Pt wire with a diameter of 25 μm sealed in a glass capillary. The measurements were carried out under normal atmosphere using a CHI 900 scanning electrochemical microscope (CH Instruments, TX, USA). The tip was characterized using ferrocene-

[z] E-mail: kontturi@cc.hut.fi

methanol as a mediator. The potential of the tip was held at 0.45 V in the approach curve measurements. The current was diffusion limited at this potential.

The copper materials used in this study were OF-HC (<10 ppm oxygen) and CuAg (2 wt % Ag) and were received from Outokumpu Copper. The substrates were placed in a Teflon holder and inserted on the bottom of the SECM cell. Na_2SO_4 (Merck, p.a.) was used as base electrolyte and ferrocenemethanol as a redox mediator (Aldrich). BTAH (Merck, p.a.) was used as the corrosion inhibitor. All solutions were prepared in Milli-Q water (Millipore). The measurements were made both in absence (1 mM FcMeOH + 100 mM Na_2SO_4) and presence of BTAH (0.667 mM FcMeOH + 67 mM Na_2SO_4 + 0.333 mM BTAH).

The measurement sequence was carried out at three different potentials of the substrate: open-circuit potential (OCP), −0.05 V, and −0.20 V: and consisted of the following steps: (1) polishing of the tip and substrate, (2) recording of an approach curve to a clean copper surface at the selected potential, and (3) recording of approach curves in the presence of BTAH after appropriate exposure times at the selected potential.

Step 1. The substrates were polished both mechanically and electrochemically prior to each measurement sequence. The mechanical polishing was done first using sandpaper (grit 600), then polishing cloth and alumina (particle size 0.3 μm), and finally using only polishing cloth and water. Electropolishing was done after the mechanical polishing in a solution of concentrated sulfuric and phosphoric acid (5 V, 2 min 77% H_3PO_4, 11.5% H_2SO_4, 11.5% H_2O by volume). The copper substrate was used as the anode and a copper sheet was used as the cathode. After electropolishing the copper substrate was cleaned in an ultrasonic bath in Milli-Q water for 15 min and twice in ethanol for 20 min.

Steps 2 and 3. An approach curve was measured first in the absence of BTAH. Then, without moving the position of the tip in the horizontal plane, the solution was changed to the BTAH-containing solution and the approach curves were measured after exposure times of 3 s, 10 min, 30 min, 1 h, 2 h, 3 h, and 4 h. The times given correspond to the exposure times before the approach curve measurements were initiated, and each approach curve measurement took approximately 1.5 min. With this procedure the approach curves were measured on the same spot of the surface, both in presence and absence of the BTAH, and therefore, effects of surface roughness of the substrate were minimized.

The approach curves were modeled assuming that the reduction of the ferrocenemethanol mediator at the copper surface was under kinetic control, as described previously (Appendix).[21,34-36] The modeling parameters were the distance between the tip and the copper surface, d, the limiting current when the tip is far away from the surface, i_{lim}, and the dimensionless heterogeneous rate constant of the reduction of the mediator at the substrate surface, $K_{S,f}$. The approach curves were drawn using the dimensionless current ($I = i/i_{lim}$) and dimensionless distance between the tip and the copper surface ($L = d/a$), where a is the radius of the tip (12.5 μm).

The thickness of the [Cu(I)–BTA] film can be calculated assuming that it is the only factor that affects the electron transfer rate constant between the bulk metal and the mediator molecule.[21] Metikoš–Huković et al.[7] estimated that the ionic diffusion coefficient in the [Cu(I)–BTA] film is approximately 4×10^{-14} cm^2 s^{-1}. According to Beverskog et al.,[37] the ratio of the electronic and ionic diffusion coefficients at room temperature is 10^5; thus, the electronic diffusion coefficient in the film is approximately 4×10^{-9} cm^2 s^{-1}. This value was used in the calculations. The diffusion coefficient of ferrocenemethanol in water was taken as 6.7×10^{-6} cm^2 s^{-1}.[38]

XPS measurements.— The OF-HC and CuAg (1 wt % Ag) samples were analyzed by X-ray photoelectron spectroscopy (XPS). The XP spectra were acquired with a Kratos XSAM-800 photoelectron spectrometer with a base pressure below 1×10^{-8} Torr (1 Torr = 133 Pa). Nonmonochromatic Mg Kα or Al Kα radiation

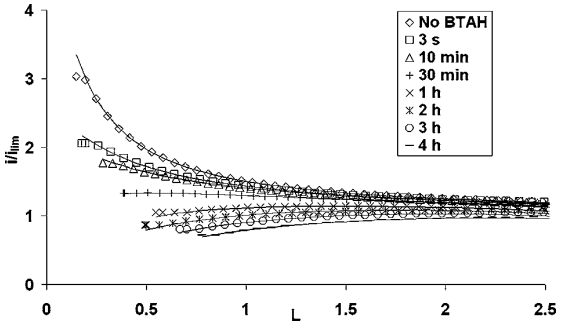

Figure 1. Approach curves of OF-HC copper measured at the substrate potential of OCP. i/i_{lim} is the dimensionless tip current, and $L = d/a$ is the dimensionless distance between the sample and the tip.

(1253.6 or 1486.6 eV) was used as a primary excitation. The hemispherical energy analyzer was operated in a fixed analyzer transmission (FAT) mode with a pass energy of 20 eV. The metallic component of Cu $2p_{3/2}$ line at 932.7 eV was used as a binding energy reference. All binding energies quoted in this work were measured within a precision of ±0.2 eV. The inelastic background was removed from the spectra using Shirley's method.[39]

The samples were cleaned in an ultrahigh vacuum (UHV) environment by Ar^+ sputtering and annealing for 15 min at 700 K. First, XP spectra of cleaned and annealed samples were measured, after which the samples were exposed to normal atmospheric pressure for 10 min and analyzed again by XPS. This was done to determine the degree of oxidation reached in 10 min. The samples were cleaned again by Ar^+ sputtering and annealing as described before, and exposed to atmospheric pressure for 10 min. The samples were then immersed in 0.33 mM BTAH aqueous solution at room temperature for 4 h. Then the samples were rinsed with distilled water and dried overnight, and finally the XP spectra of BTAH-treated samples were obtained. Additionally, the samples were Ar^+-ion-sputtered for 30 s and once again analyzed by XPS.

Results and Discussion

When a potential step is applied to a microelectrode, in this case the SECM tip, a steady-state current is quickly obtained. However, when an insulating surface is approached in a SECM measurement, the diffusion field surrounding the tip is hindered and the tip current decreases. This is typical for an insulating surface. On the contrary, an increase in the current is observed when a conductor is approached, because the redox mediator is regenerated at the surface.

Figure 1-3 show the approach curves measured at an OF-HC

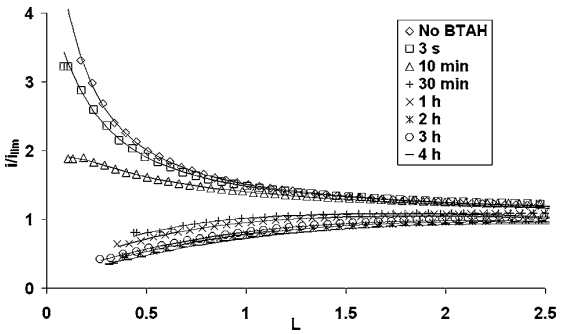

Figure 2. Approach curves of OF-HC copper measured at the substrate potential of −0.05 V vs SCE. i/i_{lim} is the dimensionless tip current, and $L = d/a$ is the dimensionless distance between the sample and the tip.

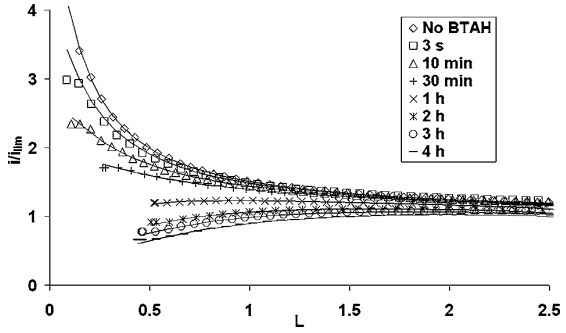

Figure 3. Approach curves of OF-HC copper measured at the substrate potential of −0.20 V vs SCE. i/i_{lim} is the dimensionless tip current, and $L = d/a$ is the dimensionless distance between the sample and the tip.

copper surface at substrate potentials of OCP, −0.05 V, and −0.20 V, respectively. The solid lines in the figures are fits and the dots are experimental results. In the absence of BTAH the current increases strongly as the tip approaches the surface. The increase is due to the regeneration of the mediator at the substrate and is typical for conductive surfaces. The approach curves in the absence of BTAH are independent of the exposure times used in this study (results not shown), indicating that copper oxide films do not interfere with the SECM response assigned to the formation of the inhibiting [Cu(I)–BTA] film.

The effect of BTAH is clearly observed as an inhibition of the rate of regeneration of the redox mediator. At short exposure times, the current increases as the surface is approached; however, in approach curves made after longer BTAH exposure times, the increase transforms into a decrease in current, indicating that the copper surface gradually changes from conductive to insulating with the growth of the inhibitive [Cu(I)–BTA] film. The rate of film growth is fastest at −0.05 V and slowest for −0.2 V, while at open-circuit potential (OCP) it is faster than at −0.2 V, but slower than at −0.05 V (see Table I for quantitative information obtained from the model). The OCP for both materials in the absence of BTAH varied between −0.02 and 0 V during the first 10 min. The OCP in the presence of BTAH was initially −0.01–0.01 V but reached a value 0.03–0.05 V after 4 h exposure. It is not clear why the film formation was slower at OCP than at −0.05 V, although the potential was more positive.

Faster inhibition at more positive potentials agrees well with the findings of Yao et al.,[15] who reported that BTAH is adsorbed on the copper surface at negative potentials, while formation of the [Cu(I)–BTA] film takes place at more positive potentials. The results for OF-HC copper are similar to what we have found previously for DHP copper;[21] however, the potential has stronger influence on DHP copper than on OF-HC copper. DHP stays conductive even after 4 h of exposure to the BTAH solution at −0.20 V,[21] indicating that the passivating [Cu(I)–BTA] film does not form. In contrast, on OF-HC copper the [Cu(I)–BTA] film still grows at the same potential (Fig. 3), reaching an estimated thickness of 20 nm in 4 h.

Figure 4-6 show the approach curves of CuAg at potentials OCP, −0.05 V, and −0.20 V, respectively. Surprisingly, the surface remains ideally conductive even after 4 h of exposure to BTAH at all potentials. We believe that this stems from the enrichment of silver at the substrate surface during the electropolishing procedure, in

Table I. The rate constants of the reduction of ferrocenementhanol at substrate surface and the thickness of [Cu(I)–BTA] films calculated using rate constants and electronic diffusion coefficient. OCP values during the film formation are shown in parenthesis below the *k* or δ values.

OF-HC	*k* (cm/s) OCP	*k* (cm/s) −0.05 V	*k* (cm/s) −0.20 V	δ (nm) OCP	δ (nm) −0.05 V	δ (nm) −0.20 V
No BTAH	0.038	0.045	0.041	1.0	0.9	1.0
3 s	0.018 (−0.01 V)	0.030	0.030	2.3 (−0.01 V)	1.3	1.3
10 min	0.014 (0.03 V)	0.014	0.019	2.8 (0.03 V)	2.9	2.1
30 min	0.008 (0.04 V)	0.003	0.013	5.2 (0.04 V)	13.8	3.0
1 h	0.004 (0.04 V)	0.002	0.006	10.2 (0.04 V)	16.6	6.9
2 h	0.003 (0.03 V)	0.001	0.003	14.1 (0.03 V)	28.5	12.1
3 h	0.002 (0.03 V)	0.002	0.003	19.2 (0.03 V)	25.1	15.1
4 h	0.001 (0.03 V)	0.001	0.002	27.8 (0.03 V)	35.5	19.7
CuAg						
No BTAH	10.518	6.904	10.627	0.7	1.1	0.7
3 s	16.251 (0.01 V)	15.734	15.904	0.5 (0.01 V)	0.5	0.5
10 min	7.259 (0.04 V)	6.397	12.116	1.0 (0.04 V)	1.2	0.6
30 min	11.138 (0.04 V)	10.235	9.139	0.7 (0.04 V)	0.7	0.8
1 h	11.149 (0.05 V)	11.219	11.984	0.7 (0.05 V)	0.7	0.6
2 h	7.344 (0.05 V)	6.488	8.922	1.0 (0.05 V)	1.2	0.8
3 h	7.183 (0.05 V)	8.898	10.807	1.0 (0.05 V)	0.8	0.7
4 h	8.110 (0.05 V)	8.059	8.638	0.9 (0.05 V)	0.9	0.9

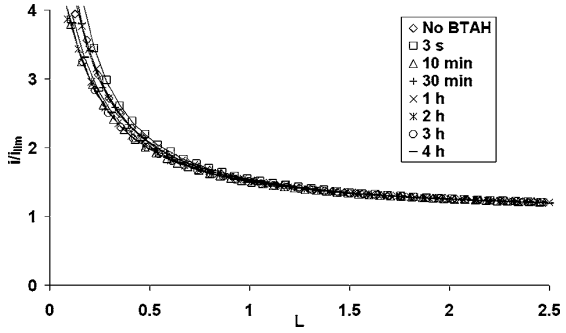

Figure 4. Approach curves of CuAg measured at the substrate potential of OCP. i/i_{lim} is the dimensionless tip current, and $L = d/a$ is the dimensionless distance between the sample and the tip.

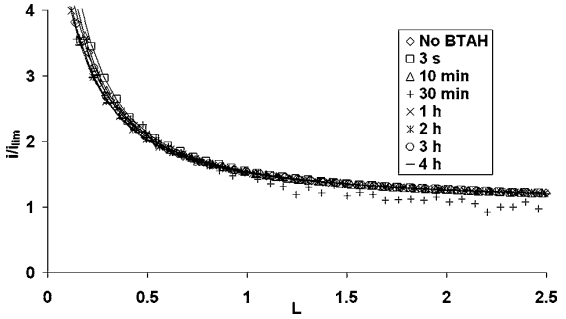

Figure 6. Approach curves of CuAg measured at the substrate potential of −0.20 V vs SCE. i/i_{lim} is the dimensionless tip current, and $L = d/a$ is the dimensionless distance between the sample and the tip.

which Cu is likely to dissolve from the surface more readily than silver. Due to the higher redox potential of silver oxidation does not take place, and consequently, the insulating BTAH film cannot form. This hypothesis is supported by the approach curves to CuAg that has not been subjected to electropolishing (see Fig. 7). In this case, growth of a protective film similar to that of OF-HC and DHP copper is observed. Recent XPS studies of the initial stages of oxidation of CuAg and OF-HC have shown that copper segregates to the surface of CuAg when it is oxidized, and furthermore, that in the end of oxidation there is no difference in the surface structure of OF-HC and CuAg.[40] Thus, the [Cu(I)–BTA] film is expected to grow similarly both on OF-HC and CuAg surfaces. We have previously shown that oxygen has a crucial role in the formation of the [Cu(I)–BTA] film.[30]

Table I shows the rate constants of ferrocenemethanol reduction on OF-HC and CuAg copper surfaces and the corresponding thickness of the films estimated using the electronic diffusion coefficient. After 4 h of exposure the thickness of the [Cu(I)–BTA] film on the OF-HC surface was 28 nm at OCP, 36 nm at −0.05 V, and 20 nm at −0.20 V. For CuAg the calculated film thickness varied around 1 nm independently of the applied potential if the electropolishing was done, and without electropolishing the thickness reached 18 nm at OCP. The thickness of the [Cu(I)–BTA] films have previously been reported to vary between 1 and 200 nm.[7,41,42] The average relative errors of the model fits typically vary in the 0–2% range. The fit corresponding to CuAg at −0.20 Vafter 30 min of exposure is poorer (5%) due to noise in the measurement (see Fig. 6).

The XP spectra of the samples are shown in Fig. 8-12. The spectra of the OF-HC sample are illustrated in solid lines and the ones of CuAg in dashed lines. The upmost pairs of spectra (a) are obtained on the samples after 10 min oxidation in normal atmospheric pressure, the ones in the middle (b) after treatment in BTAH solution, and the lowermost spectra (c) after sputtering the BTAH-treated samples.

The surface concentrations of the elements on the air/BTAH-exposed samples are listed in Table II. After air exposure, copper was found to be partly metallic and partly in the form of Cu_2O on both samples. No CuO was detected, based on the binding energies of the Cu $2p_{3/2}$ peak components and the missing shake-up structure.[43] The degree of copper oxidation was a little less on CuAg than on OF-HC. On BTAH-treated samples, a third component is detected on the Cu $2p_{3/2}$ spectra at a binding energy of 934.8 eV (Fig. 8), which is likely to originate from [Cu(I)–BTA] surface polymer.[44,45] The presence of [Cu(I)–BTA] is also confirmed by an increased intensity in Cu LMM spectra (Fig. 9) at a kinetic energy of 914.8 eV.[46]

From the O 1s spectra (Fig. 10) it can be seen that there are at least three different oxygen-containing compounds present on the sample. The two oxygen species on air-exposed samples can be characterized to be in a form of Cu_2O and oxidized carbon compounds.[43] On the BTAH-treated samples, and to a lesser extent on BTAH-treated sputtered samples, there is a third component that can be associated with partly oxidized BTAH-like compounds, or even water trapped beneath the surface polymer layer during film formation.[46]

On the air-oxidized samples, no nitrogen was detected. On BTAH-treated samples the N 1s peak (Fig. 11) is located at a binding energy of 399.7 eV. The binding energy of 399.7 eV matches with nitrogen bound to phenyl groups or conjugated nitrogen.[44] This particular peak can thus be associated with nitrogen in

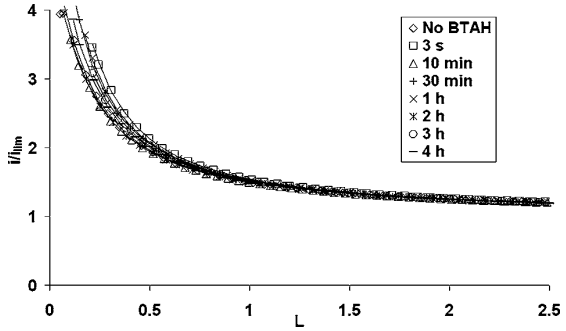

Figure 5. Approach curves of CuAg measured at the substrate potential of −0.05 V vs SCE. i/i_{lim} is the dimensionless tip current, and $L = d/a$ is the dimensionless distance between the sample and the tip.

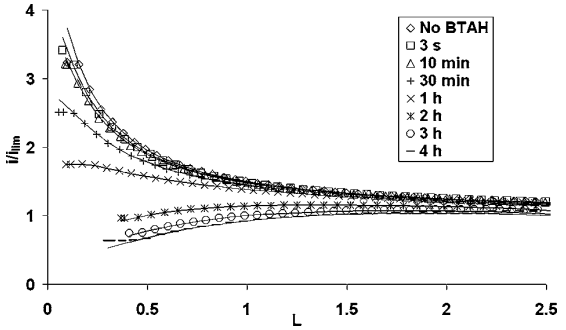

Figure 7. Approach curves of CuAg measured at the substrate potential of OCP without electropolishing. i/i_{lim} is the dimensionless tip current, and $L = d/a$ is the dimensionless distance between the sample and the tip.

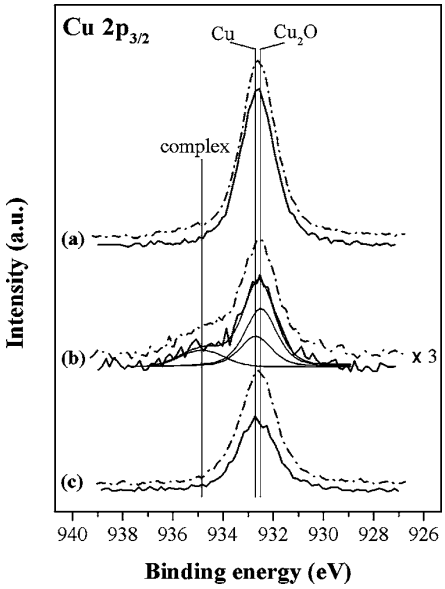

Figure 8. The XP spectra of the Cu $2p_{3/2}$ peak. Solid line spectra are obtained on the OF-HC sample and the dashed line indicates the CuAg sample. The spectra of air-exposed samples (a) are uppermost, in the middle the ones of BTAH-treated samples (b), and lowermost are the spectra of BTAH-treated, sputtered samples (c). Intensity of the spectrum pair (b) is multiplied by 3 for better comparability. The peak-fitting is accomplished with three components representing copper in metallic Cu (932.7 eV), Cu_2O (932.5 eV), and Cu–BTAH complex (934.8 eV).[43-45]

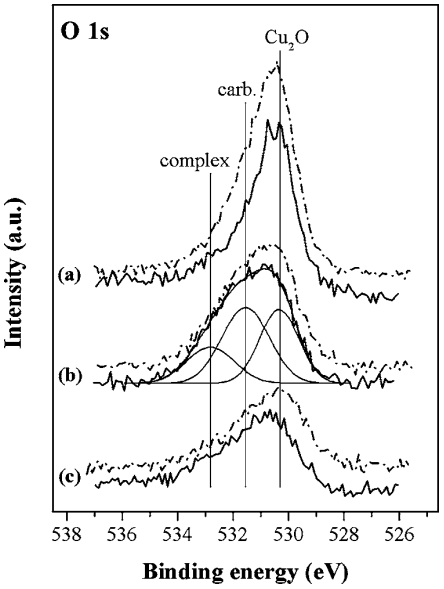

Figure 10. The XP spectra of O 1s peak. Solid line spectra are obtained on the OF-HC sample and the dashed line indicates the CuAg sample. The spectra of air-exposed samples (a) are uppermost, in the middle the ones of BTAH-treated samples (b), and lowermost are the spectra of BTAH-treated, sputtered samples (c). The peak-fitting is accomplished with three components representing oxygen in Cu_2O (530.3 eV), oxidized carbon compounds (531.7 eV) and partly oxidized BTAH-like compounds (532.8 eV).[43,46]

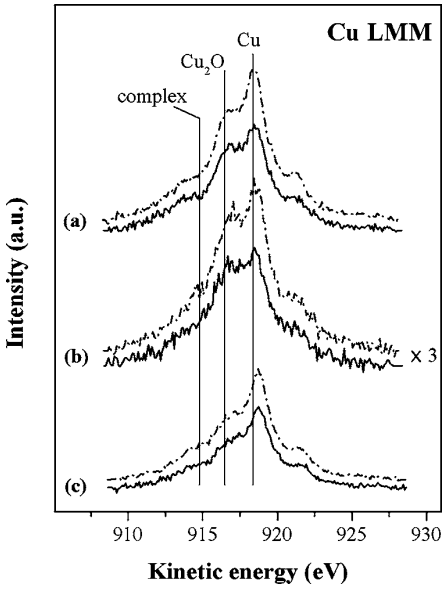

Figure 9. X-ray induced Auger Cu LMM transitions of the samples. Solid line spectra are obtained on the OF-HC sample and the dashed line indicates the CuAg sample. The spectra of air-exposed samples (a) are uppermost, in the middle the ones of BTAH-treated samples (b), and lowermost are the spectra of BTAH-treated, sputtered samples (c). Intensity of the spectrum pair (b) is multiplied by 3 for better comparability.

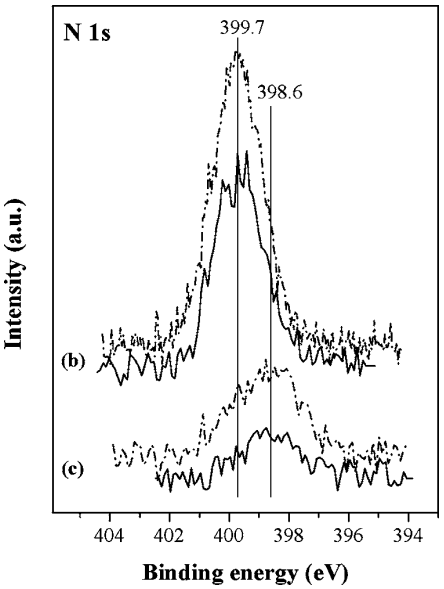

Figure 11. The XP spectra of N 1s peak. Solid line spectra are obtained on the OF-HC sample and the dashed line indicates the CuAg sample. Upper spectrum pair was measured after BTAH treatment (b) and lower pair after subsequent sputtering (c). No nitrogen was detected on the air-oxidized samples.

Table II. Binding energies of the synthetic components and relative atomic concentrations of the elements. The 10 min oxidized samples are marked as (a), BTAH-treated as (b), and BTAH treated, sputtered samples as (c).

Sample	Element	Binding energies (eV)	Compounds	Conc. (atom %)
OF-HC (a)	Cu	932.5 (63%)	Cu_2O	57
		932.7 (37%)	Cu	
	O	530.4	Cu_2O	37
		532.1	Oxidized carbon compounds	
	C	284.6	Adventitious carbon	6
OF-HC (b)	Cu	932.5 (54%)	Cu_2O	14
		932.7 (29%)	Cu	
		934.8 (17%)	Cu–BTAH complex	
	O	530.3	Cu_2O	43
		531.6	Oxidized carbon compounds	
		532.8	Oxidized BTAH	
	C	284.5	Adventitious carbon	20
		286.0	BTAH	
	N	399.7	BTAH	23
OF-HC (c)	Cu	932.5 (48%)	Cu_2O	43
		932.7 (51%)	Cu	
		934.8 (<1%)	Cu–BTAH complex	
	O	530.3	Cu_2O	34
		531.6	Oxidized carbon compounds	
		533.0	Oxidized BTAH	
	C	284.5	Adventitious carbon	15
		286.2	BTAH	
	N	398.6	BTAH	8
CuAg (a)	Cu	932.5 (51%)	Cu_2O	52
		932.7 (49%)	Cu	
	Ag	368.3	Metallic Ag	2
	O	530.4	Cu_2O	42
		531.9	Oxidized carbon compounds	
	C	284.6	Adventitious carbon	5
CuAg (b)	Cu	932.5 (43%)	Cu_2O	15
		932.7 (38%)	Cu	
		934.8 (20%)	Cu–BTAH complex	
	Ag	368.2	Metallic Ag	1
	O	530.4	Cu_2O	36
		531.8	Oxidized carbon compounds	
		532.9	Oxidized BTAH	
	C	284.5	Adventitious carbon	22
		286.2	BTAH	
	N	399.7	BTAH	26
CuAg (c)	Cu	932.5 (51%)	Cu_2O	43
		932.7 (48%)	Cu	
		934.8 (<1%)	Cu–BTAH complex	
	Ag	368.2	Metallic Ag	2
	O	530.3	Cu_2O	25
		531.7	Oxidized carbon compounds	
		532.9	Oxidized BTAH	
	C	284.5	Adventitious carbon	18
		286.2	BTAH	
	N	398.7	BTAH	12

[Cu(I)–BTA]. Sputtering the BTAH-treated samples seems to alter the chemical state of nitrogen, as indicated by the N 1s peak at a binding energy of 398.6 eV, which suggests the presence of pyridinic nitrogen[47] or nitrogen in copper–hydrocarbon complexes.[48] Although sputtering quickly reduced the amount of nitrogen, it was not easily removed from the sample completely.

Before exposing the CuAg sample to air/BTAH, the surface concentration of Ag was observed to be 5.0–5.6 atom %. The binding energy of Ag $3d_{5/2}$ was 368.1–368.2 eV on the cleaned annealed surface corresponding to metallic silver.[43] After air exposure, the Ag $3d_{5/2}$ peak had shifted to a slightly greater binding energy of 368.3 eV (Fig. 12). This binding energy shift can be associated with the increasing alloying of silver and copper as the copper segregates to the surface during oxidation.[43] On the BTAH-treated samples, the binding energy of Ag $3d_{5/2}$ was 368.2 eV, which suggests that silver is in its metallic state and has not formed oxides on the surface on any of the samples. Although, the binding energy in Ag(I)–BTA is unknown, we believe that this also rules out the existence of Ag(I)–BTA species on the sample surface. The amount of silver on the sample surface varies during oxidation and BTAH treatment, which can be observed by Ag/Cu ratio. After cleaning and annealing, the Ag/Cu ratio was 0.053, and after 10 min oxidation it had decreased to 0.037. This is likely due to the oxygen-induced surface segregation of copper. However, after BTAH treatment, the ratio was greater than on the cleaned sample, 0.072. After 30 s sputtering the ratio had decreased to 0.046. This suggests that either the surface segregation of silver is stronger in BTAH solution than on clean surface, or that some copper has dissolved from the surface during the formation of [Cu(I)–BTA] polymeric film. The latter mecha-

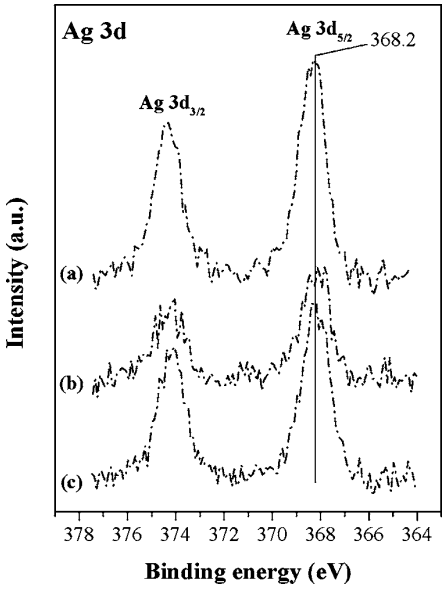

Figure 12. The Ag 3d XP spectra of the CuAg sample. The spectrum of air-exposed sample (a) is uppermost, in the middle the one of BTAH-treated sample (b), and lowermost is the spectrum of BTAH-treated, sputtered sample (c).

nism has been observed in BTAH-containing chloride solutions.[20] Considering that no interactions between BTAH and silver were observed in the XP spectra, we conclude that dissolution of copper is more likely.

Conclusions

The formation of inhibitive benzotriazole films on copper and copper alloyed with silver has been studied with XPS and SECM. The SECM results show that on OF-HC copper the film grows more rapidly with increasing potential, i.e., it was fastest at −0.05 V and slowest at −0.20 V. At OCP the rate of film formation is slightly lower than at −0.05 V. The [Cu(I)–BTA] film grows readily on CuAg that has not been electropolished. However, on the electropolished CuAg the inhibitive [Cu(I)–BTA] film does not grow independently of the applied potential, even after 4 h of exposure to BTAH. This was explained by the preferential dissolution of copper during the electropolishing procedure, leaving a surface enriched in silver.

XPS analyses of OF-HC and CuAg samples show that the Cu_2O layer formed during 10 min air exposure is partially consumed during subsequent immersion in BTAH aqueous solution, as the inhibitive surface polymer film is formed. The presence of [Cu(I)–BTA] film is indicated by Cu $2p_{3/2}$, Cu LMM, and N 1s spectra. BTAH treatment of the CuAg sample resulted in increased surface concentration of silver. No change can be seen in the binding energy of Ag $3d_{5/2}$, indicating that BTAH preferentially binds to the surface through copper.

The SECM and XPS results show that Ag has an inhibitive effect on the formation of insulating film on the copper surface.

Acknowledgments

The authors acknowledge TEKES (Technology Agency of Finland) and Outokumpu Research Oy (ORC) for funding and support.

Helsinki University of Technology assisted in meeting the publication costs of this article.

Appendix

Equations Used in the Modeling of SECM Results[21,34-36]

Equations A-1 and A-2 give the dimensionless current of the tip, when the substrate is ideally insulating or ideally conductive, respectively[34]

$$I_T^{\text{ins}} = \frac{1}{0.15 + \frac{1.5358}{L} + 0.58\exp\left(\frac{-1.14}{L}\right) + 0.0908\exp\left(\frac{L-6.3}{1.017\times L}\right)} \quad [A\text{-}1]$$

$$I_T^{\text{con}} = \frac{0.78377}{L} + 0.3315\exp\left(\frac{-1.0672}{L}\right) + 0.68 \quad [A\text{-}2]$$

T in the equations denotes the tip; con denotes a conductive and ins an insulating substrate. The dimensionless distance is defined as $L = d/a$, and the dimensionless current is defined as $I = i/i_{\text{lim}}$, where i_{lim} is the diffusion limiting current of the mediator on a disk ultramicroelectrode placed at an infinite distance from the substrate[34]

$$i_{\text{lim}} = 4nFDca \quad [A\text{-}3]$$

When the reaction at the substrate is under kinetic control, the dimensionless tip and substrate currents can be related by Eq. A-4[36]

$$I_T = I_S^k\left(1 - \frac{I_T^{\text{ins}}}{I_T^{\text{con}}}\right) + I_T^{\text{ins}} \quad [A\text{-}4]$$

where

$$I_S^k = \frac{0.78377}{L(1 + 1/\Lambda)} + \frac{0.68 + 0.3315\exp\left(\frac{-1.0672}{L}\right)}{1 + \frac{11/\Lambda + 7.3}{\Lambda(110 - 40L)}} \quad [A\text{-}5]$$

S denotes the substrate and superscript k kinetic control of the reaction. Λ is defined by Eq. A-6[35]

$$\Lambda = \frac{k_{S,f}d}{D_R} = K_{S,f}L \quad [A\text{-}6]$$

$K_{S,f}$ denotes the dimensionless heterogeneous rate constant at the substrate surface[36]

$$K_{S,f} = \frac{ak_{S,f}}{D_R} \quad [A\text{-}7]$$

A rough estimate of the changes in the thickness of the film can be also calculated as a function of time, if the thickness is assumed to be the only factor that influences the changes of the film resistance. In these cases the apparent $k_{S,f}$ can be defined as

$$k_{S,f} = \frac{D_{\text{film}}}{\delta} \quad [A\text{-}8]$$

References

1. J. R. Davis and P. Allen, *Metals Handbook*, Vol. 2, pp. 230, 265–267, 10th ed., ASM International (1990).
2. C. H. Brooks, *Heat Treatment, Structure and Properties of Nonferrous Alloys*, p. 275 and 285, American Society for Metals, Materials Park, OH (1982).
3. W. Qafsaoui, Ch. Blanc, N. Pébère, A. Srhiri, and G. Mankowski, *J. Appl. Electrochem.*, **30**, 959 (2000).
4. D. Tromans, *J. Electrochem. Soc.*, **145**, L42 (1998).
5. P. Yu, D.-M. Liao, Y.-B. Luo, and Z.-G. Chen, *Corrosion (Houston)*, **59**, 314 (2003).
6. E. M. M. Sutter, F. Ammeloot, M. J. Pouet, C. Fiaud, and R. Couffignal, *Corros. Sci.*, **41**, 105 (1999).
7. M. Metikoš-Huković, R. Babić, and I. Paić, *J. Appl. Electrochem.*, **30**, 617 (2000).
8. V. Brusic, M. A. Frisch, B. N. Eldridge, F. B. Novak, F. B. Kaufman, B. M. Rush, and G. S. Frankel, *J. Electrochem. Soc.*, **138**, 2253 (1991).
9. K. Cho, J. Kishimoto, T. Hashizume, H. W. Pickering, and T. Sakurai, *Appl. Surf. Sci.*, **87/88**, 380 (1995).
10. B.-S. Fang, C. G. Olson, and D. W. Lynch, *Surf. Sci.*, **176**, 476 (1986).
11. J.-O. Nilsson, C. Törnkvist, and B. Liedberg, *Appl. Surf. Sci.*, **37**, 306 (1989).
12. O. Hollander and R. May, *Corrosion (Houston)*, **41**, 39 (1985).
13. J. F. Walsh, H. S. Dhariwal. A. Gutiérrez-Sosa, P. Finetti, C. A. Muryn, N. B. Brookes, R. J. Oldman, and G. Thornton, *Surf. Sci.*, **415**, 423 (1998).
14. R. Youda, H. Nishihara, and K. Aramaki, *Electrochim. Acta*, **35**, 1011 (1990).
15. J.-L. Yao, Y.-X. Yuan, and R.-A. Gu, *J. Electroanal. Chem.*, **573**, 255 (2004).
16. P. G. Gao, J. L. Yao, W. Zheng, R. A. Gu, and Z. Q. Tian, *Langmuir*, **18**, 100 (2002).
17. H. Y. H. Chan and M. J. Weaver, *Langmuir*, **15**, 3348 (1999).
18. Z. D. Schultz, M. E. Biggin, J. O. White, and A. A. Gewirth, *Anal. Chem.*, **76**, 604 (2004).
19. G. M. Brisard, J. D. Rudnicki, F. McLarnon, and E. J. Cairns, *Electrochim. Acta*, **40**, 859 (1995).
20. D. Tromans and R. Sun, *J. Electrochem. Soc.*, **138**, 3235 (1991).
21. K. Mansikkamäki, P. Ahonen, L. Murtomäki, G. Fabricius, and K. Kontturi, *J. Electrochem. Soc.*, **152**, B12 (2005).
22. S. Kapoor, *Langmuir*, **14**, 1021 (1998).
23. S. Thomas, S. Venkateswaran, S. Kapoor, R. D'Cunha, and T. Mukherjee, *Spec-*

trochim. Acta, Part A, **60**, 25 (2004).
24. S. Naumov, S. Kapoor, S. Thomas, S. Venkteswaran, and T. Mukherjee, *J. Mol. Struct.: THEOCHEM*, **685**, 127 (2004).
25. E. Ahn and J. J. Kim, *Electrochem. Solid-State Lett.*, **7**, C118 (2004).
26. I. Serebrennikova and H. S. White, *Electrochem. Solid-State Lett.*, **4**, B4 (2001).
27. I. Serebrennikova, S. Lee, and H. S. White, *Faraday Discuss.*, **121**, 199 (2002).
28. S. B. Basame and H. S. White, *J. Phys. Chem. B*, **102**, 9812 (1998).
29. S. B. Basame and H. S. White, *Anal. Chem.*, **71**, 3166 (1999).
30. K. Mansikkamäki, C. Johans, and K. Kontturi, *J. Electrochem. Soc.*, **153**, B22 (2006).
31. C. Jin-Hua, L. Zhi-Cheng, C. Shu, N. Li-Hua, and Y. Shou-Zhuo, *Electrochim. Acta*, **43**, 265 (1998).
32. F. M. Al-Kharafi and B. G. Ateya, *J. Electrochem. Soc.*, **149**, B206 (2002).
33. Z. Xu, S. Lau, and P. W. Bohn, *Langmuir*, **9**, 993 (1993).
34. A. J. Bard, F.-R. F. Fan, and M. V. Mirkin, in *Electroanalytical Chemistry*, A. J. Bard, Editor, p. 243, Marcel Dekker, Inc., New York (1994).
35. K. Bogwarth and J. Heinze, in *Scanning Electrochemical Microscopy*, A. J. Bard and M. V. Mirkin, Editors, p. 201, Marcel Dekker, Inc., New York, (2001).
36. M. V. Mirkin, in *Scanning Electrochemical Microscopy*, A. J. Bard and M. V. Mirkin, Editors, p. 145, Marcel Dekker, Inc., New York (2001).
37. B. Beverskog, M. Bojinov, P. Kinnunen, T. Laitinen, K. Mäkelä, and T. Saario, *Corros. Sci.*, **44**, 1923 (2002).
38. N. Anicet, C. Bourdillon, J. Moiroux, and J.-M. Savéant, *J. Phys. Chem. B*, **102**, 9844 (1998).
39. D. A. Shirley, *Phys. Rev. B*, **5**, 4709 (1972).
40. M. Hirsimäki, M. Lampimäki, K. Lahtonen, I. Chorkendorff, and M. Valden, *Surf. Sci.*, **583**, 157 (2005).
41. R. Babić, M. Metikoš-Huković, and M. Lončar, *Electrochim. Acta*, **44**, 2413 (1999).
42. A. Frignani, M. Fonsati, C. Monticelli, and G. Brunoro, *Corros. Sci.*, **41**, 1217 (1999).
43. J. F. Moulder, W. F. Stickle, P. E. Sobol, and K. D. Bomben, *Handbook of X-Ray Photoelectron Spectroscopy*, Perkin-Elmer Corporation, Eden Prairie, MN (1992).
44. D. Chadwick and T. Hashemi, *Corros. Sci.*, **18**, 39 (1978).
45. D. Chadwick and T. Hashemi, *J. Electron Spectrosc. Relat. Phenom.*, **10**, 79 (1977).
46. L. Tommesani, G. Brunoro, A. Frignani, C. Monticelli, and M. Dal Colle, *Corros. Sci.*, **39**, 1221 (1997).
47. Z. Zude, Z. Xiong, Z. Tao, Y. Huaming, and L. Qingliang, *J. Mol. Struct.*, **478**, 23 (1999).
48. J. Lahaye, G. Nansé, A. Bagreev, and V. Strelko, *Carbon*, **37**, 585 (1999).